



Research Article

Effects of Electrode Location on Estimates of Neural Health in Humans with Cochlear Implants

KARA C. SCHVARTZ-LEYZAC,^{1,2,3}  TIMOTHY A. HOLDEN,⁴ TERESA A. ZWOLAN,² H. ALEXANDER ARTS,² JILL B. FIRSZT,⁴ CHRISTOPHER J. BUSWINKA,¹ AND BRYAN E. PFINGST¹

¹*Kresge Hearing Research Institute, Department of Otolaryngology, Michigan Medicine, 1150 West Medical Center Drive, Ann Arbor, MI 48109-5616, USA*

²*Hearing Rehabilitation Center, Department of Otolaryngology, Michigan Medicine, 475 W. Market Place, Building 1, Suite A, Ann Arbor, MI 48108, USA*

³*Department of Otolaryngology, Medical University of South Carolina, 135 Rutledge Ave, MSC 550, Charleston, SC 29425, USA*

⁴*Department of Otolaryngology-Head and Neck Surgery, Washington University School of Medicine, St. Louis, MO, USA*

Received: 30 May 2019; Accepted: 24 February 2020; Online publication: 27 April 2020

ABSTRACT

There are a number of psychophysical and electrophysiological measures that are correlated with SGN density in animal models, and these same measures can be performed in humans with cochlear implants (CIs). Thus, these measures are potentially applicable in humans for estimating the condition of the neural population (so called “neural health” or “cochlear health”) at individual sites along the electrode array and possibly adjusting the stimulation strategy in the CI sound processor accordingly. Some measures used to estimate neural health in animals have included the electrically evoked compound potential (ECAP), psychophysical detection thresholds, and multipulse integration (MPI). With regard to ECAP measures, it has been shown that the change in the ECAP response as a function of increasing the stimulus interphase gap (“IPG Effect”) also reflects neural density in implanted animals. These animal studies have typically been conducted using preparations in which the electrode was in a fixed position with respect to the neural population, whereas in human cochlear implant users, the position of individual electrodes varies widely within an electrode array and also across subjects. The current study evaluated the effects of electrode location in the implanted cochlea (specifically medial-lateral location) on

various electrophysiological and psychophysical measures in eleven human subjects. The results demonstrated that some measures of interest, specifically ECAP thresholds, psychophysical detection thresholds, and ECAP amplitude-growth function (AGF) linear slope, were significantly related to the distances between the electrode and mid-modiolar axis (MMA). These same measures were less strongly related or not significantly related to the electrode to medial wall (MW) distance. In contrast, neither the IPG Effect for the ECAP AGF slope or threshold, nor the MPI slopes were significantly related to MMA or MW distance from the electrodes. These results suggest that “within-channel” estimates of neural health such as the IPG Effect and MPI slope might be more suitable for estimating nerve condition in humans for clinical application since they appear to be relatively independent of electrode position.

Keywords: cochlear implant, electrode placement, neural health

Correspondence to: Kara C. Schwartz-Leyzac · Department of Otolaryngology · Medical University of South Carolina · 135 Rutledge Ave, MSC 550, Charleston, SC 29425, USA. email: leyzac@musc.edu

INTRODUCTION

Several animal studies have demonstrated that specific electrophysiological and psychophysical measures reflect local spiral ganglion neuron (SGN) survival in cochlear-implanted animals

(Prado-Guitierrez et al., 2006; Earl and Chertoff, 2010; Pfungst et al., 2011; Ramekers et al., 2014; Pfungst et al., 2015a; Pfungst et al., 2015b; Ramekers et al., 2015; Pfungst et al., 2017; Schwartz-Leyzac et al., Submitted). Results in both acute and long-term deafened animals have demonstrated that approximately 50 % or more of the variance in suprathreshold measures (AGF linear slope and peak-amplitude) of the electrically evoked auditory brainstem response (EABR) Wave I and/or ECAP across cochlear implanted animals can be accounted for by SGN density (Smith and Simmons, 1983; Hall, 1990; Ramekers et al., 2014; Schwartz-Leyzac et al., Submitted). There is a weaker and unclear relationship between ECAP thresholds and neural density and/or health (Shepherd et al., 1993; Shepherd and Javel, 1997; Ramekers et al., 2014). Generally, ECAP amplitudes and AGF slopes increase with an increase in IPG duration (“IPG Effect”), and the increase is greater in animals with higher neural density (Ramekers et al., 2014).

Multipulse integration (MPI) is the phenomenon by which the psychophysical detection threshold improves (lowers) with increasing pulse rate, and the slope of this function has been shown to relate with attributes of cochlear health (e.g., neural density, presence/absence of hair cells, and spontaneous activity) in cochlear-implanted guinea pigs (Kang et al., 2010; Pfungst et al., 2011; Zhou et al., 2015). However, the relationship between simple psychophysical detection thresholds and neural density is not yet clear. Generally, there is not strong evidence to support a relationship between SGN density and psychophysical threshold detection for pulse trains at very low pulse rates or for single pulses (Pfungst et al., 2011; Pfungst et al., 2019) in cochlear-implanted animals. It has been hypothesized that psychophysical detection thresholds using focused stimulation reflect features of the electrode-neural interface including neural conditions (Bierer and Faulkner, 2010; Goldwyn et al., 2010), but this relationship has not yet been directly examined in an animal model.

While these electrophysiological and psychophysical measures have promise for use in CI programming, several studies produce mixed results when examining the relationship between such measures and speech recognition performance in CI listeners (Zhou and Pfungst, 2014; He et al., 2017; van Eijl et al., 2017; Schwartz-Leyzac and Pfungst, 2018). However, one factor that confounds the extrapolation of animal data to humans is that the diameter of the electrode array relative to the diameter of the scala tympani in small animal cochleae (e.g., guinea pigs) does not typically allow for significant variation in electrode to medial wall placement; studies have shown that electrode placement varies widely across human

subjects (Skinner et al., 2007; Finley et al., 2008; Teymouri et al., 2011; Long et al., 2014). Therefore, in order for these measures to be clinically applicable, it is important to understand how electrode location affects electrophysiological and psychophysical neural health measures.

DeVries et al. (DeVries et al., 2016) did not find a significant relationship between ECAP amplitude measures obtained at a moderately comfortable loudness level and distance between the electrode and the cochlear medial wall in human CI recipients. However, other studies have observed that threshold and suprathreshold ECAP measures differ at apical and basal electrode sites and have hypothesized that perhaps medial-lateral electrode distance might contribute to these observations (Nehme et al., 2014; van de Heyning et al., 2016). Shepherd et al. (1993) showed that the slope of the EABR Wave IV AGF became shallower and thresholds became lower as the position of a single recording electrode was moved closer to the modiolus in normal hearing and long-term deafened cats (Shepherd et al., 1993). This factor could confound previous studies, which show steeper EABR Wave I and ECAP AGF slopes in animals with higher neural densities. Related studies in cochlear-implanted humans suggest that psychophysical detection thresholds using focused current configurations are also related to the distance between the electrode and the medial wall (Long et al., 2014; DeVries et al., 2016). In the same study, Long et al. (2014) showed that in the same subjects, thresholds assessed using monopolar configurations were less likely to be correlated with the same distance measure.

In the present study, we examined the effects of electrode location on psychophysical and ECAP measures in human cochlear implant users. We examined distance from the electrode to the medial wall (MW) and also distance from the electrode to the mid-modiolar axis (MMA). Since neither the site of action-potential initiation nor the relative contributions of the individual spiral ganglion neurons are known, it is not obvious which of these metrics should give the best correlation with psychophysical and ECAP measures examined in the present study; therefore, both metrics are reported in the following analyses. It is possible that previous studies showing little or no relationship between cochlear health measures and medial-lateral distance using the MW estimate might indeed show a relationship when examining medial-lateral distance using the MMA measure. In theory, ECAP IPG Effect and MPI measures, which reflect neural density in cochlear-implanted animals, should be minimally influenced by non-neural factors, such as electrode distance, as these measures simply vary the IPG or the pulse rate within the same electrode and/or channel.

METHODS

Subjects

Subjects were 11 unilateral cochlear implant users with peri- or post-lingual sensorineural hearing loss. The ears were implanted with Cochlear Nucleus CI512, CI24RE(CA) or CI422 devices. Three of the subjects had measurable post-operative acoustic hearing at the time of testing. Demographic information for the subjects is shown in Table 1. Eight subjects were implanted at the University of Michigan, while three were implanted at another local cochlear implant center. The use of human subjects in the study was reviewed and approved by the University of Michigan Medical School Institutional Review Board.

Electrophysiological Measures

ECAP AGFs were measured on each available electrode in all subjects. The AGF could not be measured on some electrodes in some subjects due to any of the following reasons: deactivated electrode, restricted dynamic range (discomfort or compliance limits), or could not record a waveform with sufficient morphology (e.g., clearly identifiable and repeatable N1-P2 peaks). Table 2 provides information for each subject and identifies each electrode where an ECAP could not be recorded and states reasons for absent recordings. ECAP AGFs were not considered valid for the purpose of this study for very restricted dynamic ranges, which yielded less than 4 data points and for which a slope could not be reliably estimated (see below for further information regarding slope calculation).

ECAPs were measured using methods similar to those cited in previous studies (Schvartz-Leyzac and Pfungst, 2016, 2018). Please refer to these manuscripts for more detailed information. Briefly, ECAPs were assessed with Cochlear Corporation CustomSound® EP Versions 4.4, 4.5 or 5.1 software using Neural Response Telemetry. A laboratory-owned CP910 speech processor connected to a desktop computer through a commercially available programming pod was used for data collection. Prior to measuring AGFs, the maximum tolerable stimulation level was determined on each electrode, for each IPG condition. The measured maximum stimulation level for each electrode was used as the upper limit of stimulation when measuring the AGFs. Typically, subjects reported the maximum stimulation level as very loud but tolerable.

The “amplitude-growth function” protocol available within the clinical software was used to obtain each AGF. The limits of the dynamic range of stimulation for the AGFs differed in absolute current level for each electrode (1 = base; 22 = apex); for each

electrode, the lowest current level was insufficient to evoke a response (i.e., set below response threshold in order to obtain a “no response” waveform) and the upper limit of the dynamic range of stimulation was equal to the maximum stimulation level, as defined in the previous paragraph. The current level step size was 5 clinical units (CUs) ($\text{CU in } \mu\text{A} = 17.5 \mu\text{A} * (100^{(\text{CU}/255)})$). At least four data points were required to fit the slope function (dynamic range = 15 CU). For each recording, the peak-to-peak ECAP amplitudes were measured from the leading negative peak (N1) to the following positive peak (P2) using the CustomSound® EP software. The input-output function for each electrode was measured 2–3 times for each condition (7 and 30 μs IPGs, as outlined below).

ECAP recording parameters were identical to those described previously (Schvartz-Leyzac and Pfungst, 2016, 2018), and details are provided briefly here. A forward-masking technique was used for artifact cancellation (Abbas et al., 1999; Abbas et al., 2004). The pulse rate = 80 pps, sampling rate = 20 kHz, pulse phase duration = 25 μs , and the IPG of the biphasic pulse was either 7 or 30 μs . The MP1 electrode was the probe and masker indifferent electrode, and the MP2 electrode was the recording indifferent electrode. The probe and masker active electrodes were always co-located and the masker level was always 10 CUs higher than the probe level. The masker probe interval was 400 μs . The recording electrode was always located two electrodes apical to the probe electrode when the probe electrode varied between electrodes 1–20. When the probe electrode was 21, electrode 22 was used as the recording electrode. When the probe electrode was 22, the recording electrode was 21. The leading phase of the biphasic pulse for both the probe and the masker was always cathodic. The default gain and delay were used in most cases; however, for some electrodes, these parameters were adapted in order to improve the visibility of the N1 peak or morphology of the signal.

Psychophysical Measures

All measures were conducted using a laboratory-owned Freedom® speech processor (Cochlear Corporation, Englewood, CO), custom MATLAB® software (The Mathworks, 2010a) and the Nucleus Implant Communicator (NIC2) research tool (Cochlear Ltd). Psychophysical detection thresholds were measured using 500 ms trains of biphasic pulses at two pulse rates: 80 and 640 pps. The phase duration = 25 μs and an interphase gap = 8 μs .

First, the method of adjustment (MOA) threshold (T) levels were estimated on each electrode by increasing current level in steps of 1 or 5 clinical

TABLE 1

Demographic information for each subject. Subject s112 initially received a CI24RECA device in 2016, and after 1 year of use, post-operative imaging revealed a tip-fold over. The subject was subsequently reimplanted with a CI512 device in 2017 and had 1 year of experience with this device at the time of study participation. The pre- and post-op PTAs were calculated based on a traditional three-frequency average at 500, 1000, and 2000 Hz

Subject	Gender	Age	Onset of Hearing loss	Etiology	Ear	Years implant use	Device	Pre-op PTA (dB HL)	Post-op PTA (dB HL)
s98	M	80	20s	Otosclerosis / Noise exposure	L	5	CI24RE(CA)	NR	NR
s105	F	74	50s	Unknown	R	4	CI422	86.6	86.6
s110	F	64	49 years old	Unknown	R	2	CI24RE(CA)	110	NR
s111	M	75	2 years old	Measles	R	2	CI422	78.3	NR
s112	M	49	40s	Meniere's	R	1	CI512	93.3	NR
s113	F	76	Teenager	Hereditary	L	3	CI422	91.6	96.6
s114	F	48	7 years old	Meningitis	L	2	CI512	NR	NR
s115	M	74	40s	Noise exposure	L	3	CI422	65	NR
s116	F	38	2–3 years old	Hereditary	R	9	CI24RE(CA)	100	116.6
s117	F	38	Teenager	Hereditary	L	11	CI24RE(CA)	90	NR
s118	M	74	Teenager	Unknown	L	1	CI512	NR	NR

units (CUs) until the subject reported they were just able to hear the sound. Current level was increased by the examiner in steps of 5 CU until the subject reported the sound was loud but comfortable. The T and C levels obtained using the MOA method were then entered in a separate custom MATLAB® program to more accurately assess T levels using an adaptive three-alternative forced-choice (3AFC) method in which one interval contained a stimulus and the other two intervals contained no stimulus. Using a computer mouse and custom graphical user interface,

subjects selected the appropriate interval containing the stimulus. The initial stimulus for each electrode was presented at 50 % of the dynamic range. A two-down, one-up adaptive procedure was used with 5 CU steps for the first four reversals and 1 CU steps for the next six reversals for a total of ten reversals; the last five reversals were averaged to determine the threshold. This threshold measurement was repeated for a third time, if the second measurement was $\pm 5\%$ from the first, and in that case all three measurements were used to calculate a threshold for a given electrode.

TABLE 2

For each subject, the electrode number is indicated in which an ECAP response (threshold or AGF linear slope) could not be recorded or was not recorded (e.g., deactivated electrode in clinical map). For only one subject (s117), the IPG Effect could not be calculated for several electrodes, and therefore this subject was not included in analyses using the ECAP IPG Effect

Subject ID	Electrodes without ECAP AGF measure				IPG Effect calculated?
	7 μ s IPG		30 μ s IPG		
	Threshold	Slope	Threshold	Slope	
s98	1,2 [#]	1,2 [#]	1,2 [#]	1,2 [#]	Yes
s105	1–5 [#]	1–5 [#]	1–5 [#]	1–5 [#]	Yes
s110	1,2 [#]	1,2 [#]	1,2 [#]	1,2 [#]	Yes
	12 [^]	12 [^]	12 [^]	12 [^]	
s111	1–9 [^]	1–9 [^]	1,2,5,7,8 [^]	1–8 [^]	Yes
s112	1*	1*	1*	1*	Yes
s113	1,2 [#]	1,2 [#]	1,2 [#]	1,2 [#]	Yes
	3*	3*	3*	3*	
s114	1–3*	1–3*	1–3*	1–3*	Yes
s115	1–4, 14 [#]	1–4, 14 [#]	1–4, 14 [#]	1–4, 14 [#]	Yes
s116	N/A	8,9*	N/A	19	Yes
s117	1, 2, 3, 4, 16 [^]	1,2,3,4,16 [^]	1,2,3,4,16 [^]	1,2,3,4,16 [^]	No
		7*	7,9,10,13,15*	7,9,10,13,15*	
s118	1,2*	1,2*	1,2*	1,2*	Yes
	16–22 [^]	16–22 [^]	16–22 [^]	16–22 [^]	

[#]Disabled in clinical map

*Restricted dynamic range/discomfort

[^]Could not record waveform

Computerized Tomography

Post-operative computerized tomography (CT) scans were performed in all subjects using identical methods previously described (Skinner et al., 2007; Teymouri et al., 2011; Long et al., 2014; DeVries et al., 2016). Briefly, CT voxel space and anatomical details were optimized for electrode placement using the subject's contralateral, non-implanted ear (ANALYZE software, Mayo Clinic, Rochester, MN, USA; Robb 2001). To better visualize the scalar position of the electrode array and the individual electrode contacts, a high-resolution cochlear atlas was aligned with the CT volume to estimate the location of fine and soft tissue intra-cochlear structures. One of eleven possible atlases were matched for each subject based on the outline of the osseous features in an individual's cochlea. Three measures were used in the current study based on the CT scans, two of which have been previously described elsewhere (Long et al., 2014; DeVries et al., 2016).

The first measure ("Medial Wall", or MW) estimated the radial distance (mm) from each electrode contact to the medial wall of the cochlea (Fig. 1a, dashed line). The second measure ("Mid-modiolar axis" or MMA) refers to an axis more medial than the MW measure falling within the estimated mid-modiolar core of the cochlea (Fig. 1a, solid line). The MMA measure was derived using the following method. Each subject's cochlea in their CT volume was registered (translated and rotated) to center and align it with the cochlear canal wall boundaries of a cochlea atlas template to create a new volume with the subject's cochlea in a standardized orientation. The atlas was based on a hi-resolution (16 μm voxels) orthogonal-plane, fluorescence optical sectioning (OPFOS) microscopy scan of a single male donor

with normal cochlear anatomy that illustrates details of both the soft tissue and bony structure of the cochlea (Voie, 2002). Since an MMA of a subject's cochlea cannot solely be determined from the clinical CT images due to image resolution and poor soft tissue contrast, the MMA of the OPFOS cochlea atlas was projected into the subject's standardized volume. The standardized subject's CT volume was then used as the basis for the CI CT analysis. In order to best project the location of ST and SV in a subject's cochlea, each of 12 cochlear atlases (1 OPFOS, 11 Micro CT) were independently visually registered and scaled to the subject's cochlear canal wall boundaries to find the best match in overall cochlear shape.

The third measure ("scalar location") refers to one of three locations within the cochlea: (1) scala tympani (ST), (2) scala vestibuli (SV), and (3) medial region (M). Note that the M region does not assume that electrodes are located within the scala media but rather that, based on resolution capabilities of the CT scans, a specific location of ST or SV cannot be determined. All scans were performed at the University of Michigan Medical Center at least 12 months following cochlear implant surgery and were completed within 1 year of the ECAP recordings and psychophysical measures obtained for each subject.

Statistical Analysis

All data were analyzed using MATLAB and R Version 3.5.1 (The Mathworks, 2017; RCoreTeam, 2018). The key variables of interest for each ECAP input-output function were the ECAP AGF slopes and thresholds. It was observed that the majority of AGFs were linear; however, there were a small number of cases that demonstrated nonlinearity. In an effort to fit all data

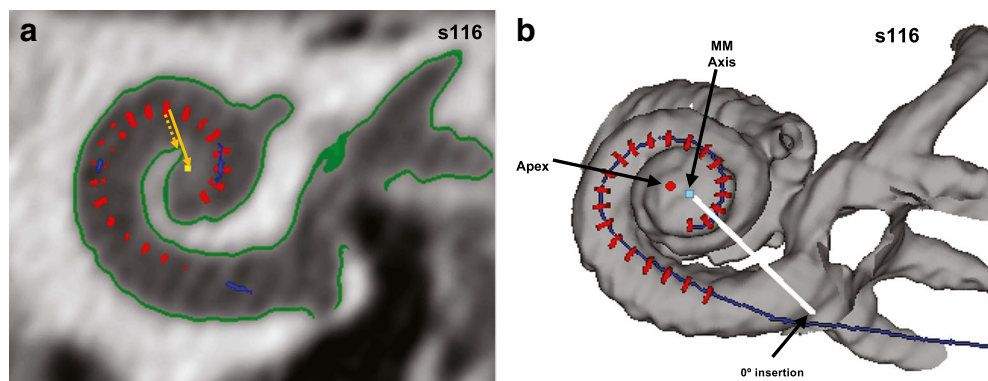


FIG. 1. **a** The distance between the electrode and the mid-modiolar axis (MMA; solid orange line) and the medial wall (MW; dashed orange line). This figure represents data obtained from s116 and represents a cross-sectional slice through the cochlea along the horizontal plane. The short red lines are schematics of the approximate electrode locations and are shown relative to the clinical CT scan. The green lines are derived from the boundaries

of fluid/tissue space of s116's cochlea and the otic bone and define the cochlear canal wall. **b** A 3D reconstructed image (s116) and demonstrates the location of the determined mid-modiolar axis (blue dot) and the apex of the cochlea (red). The end of the white line drawn from the MM Axis marks the 0° angle of rotation about the MM axis for electrode insertion angles

in the same way, the following method was used and was previously reported in a recent publication (Schvartz-Leyzac et al., 2019). All points below 5 μV (noise floor) were excluded. The AGF was linearized by approximating the slope of the linear region using the “gradient” function in MATLAB and systematically removing the points that deviated by more than 20 % of this slope. A linear model ($y = y_0 + ax$) was fit to all of the remaining points, and the resulting slope was calculated. In all cases, the linear fit was statistically significant and produced an R^2 of 0.95 or higher. The ECAP threshold was defined as the lowest level of current that evoked a response above the noise floor of the system (5 μV). ECAP thresholds were measured in CUs were converted to μA and then expressed in dB re: 1 mA. The change (increase or decrease) in slope or threshold as a function of the IPG (the “IPG Effect”) was also calculated for each electrode by subtracting the slope or threshold for the 7 μs IPG stimulus from that for the 30 μs IPG stimulus.

Multipulse integration was calculated using methods described previously (Pfungst et al., 2011; Zhou et al., 2012; Zhou and Pfingst, 2014, 2016). The T levels obtained on the 2AFC task (described above) measured in CUs for 80 and 640 pps were converted to μA and then expressed in dB re: 1 mA. The MPI slopes for each electrode, for each subject, were calculated using least-squares linear regression; T levels were expressed as dB re: 1 mA and pulse rates were transformed on a log scale (\log_2). The slope values from the regression model were used as the MPI slope values.

A linear mixed modeling approach was used to determine how ECAP and psychophysical measures were related to CT-derived measures across all subjects. Linear mixed modeling was performed using R and the “lme4” package, and p values were derived using “lmerTest” (Bates et al., 2015; Kuznetsova et al., 2017; RCoreTeam, 2018). For each ECAP and psychophysical measure, we performed linear mixed models with both the MW and MMA distances. The best model in all analyses was produced by incorporating both fixed and random effects for slope and intercept, as determined using the maximum likelihood. Models using MW and MMA distance measures were compared using the maximum likelihood test to determine if the models were significantly different from one another and if so, which provided a better fit to the data based on Akaike information criterion (AIC).

RESULTS

Electrode Locations

Analysis of CT scans revealed considerable variation of both scalar location and medial-lateral electrode position across all subjects. The across-electrode

pattern differed within each subject. Individual electrodes were classified as being in the scala tympani (ST), the M region, or in the scala vestibuli (SV). The classification for each electrode is shown by symbol shape in Figs. 2 and 3. Note that electrode numbers range from 1 (basal) to 22 (apical). For two subjects (s116 and s118), the CT analysis indicated that all electrodes were clearly in the ST. Another 5 subjects showed a mix of electrode locations in ST or the M region. For electrodes in the M region, it was not possible to tell from the CT data alone if the electrode array was just near the basilar membrane, was touching the basilar membrane, or if it had penetrated the basilar membrane. However, two subjects who had some electrodes designated as being in the M region (s105 and s113) showed long-term (> 3 years) complete preservation of pre-operative residual hearing (within 10 dB HL of pre-operative thresholds at all frequencies), and therefore it is assumed that all electrodes were located within the ST; however, this is not known with absolute certainty, and therefore they are reported as being located in the M region in this study. In one other subject (s117), all electrodes except for Electrode 1 were located within the ST. In subject s115, all electrodes were identified in the ST or M region; this subject did lose the remainder of residual hearing post-operatively. The remaining subjects (s98, s110, s111, and s114) clearly had some electrodes in ST and some in SV. Across all subjects, 16.52 %, 57.42 %, and 26.03 % of the electrodes were identified as being located in the scala vestibuli, scala tympani, and the M region, respectively.

Average values for both metrics of medial-lateral distance are provided in Table 3. For each subject, the relationship between MMA and MW distances are shown in Fig. 2. Because linear regression analyses assume independent observations, formal statistics were not performed. However, it can be observed that for some subjects (e.g., s114, s112), the MMA and MW distances are linearly related, but in most other subjects, the relationship is nonlinear. Figure 3 shows the pattern between insertion angle and either MMA or MW distance for each subject. These plots help to describe the results displayed in Fig. 2 and largely demonstrate that the MMA and MW distance measures are more parallel at deeper insertion angles and become non-linear at shallower insertion angles. Overall, these comparisons demonstrate that for most subjects the MMA and MW metrics are somewhat distinct.

Relation of Electrode Locations to Electrically Evoked Compound Action Potentials (ECAPs)

The across-site patterns of ECAP data for each subject are shown in Fig. 4c–f, and the descriptive statistics are

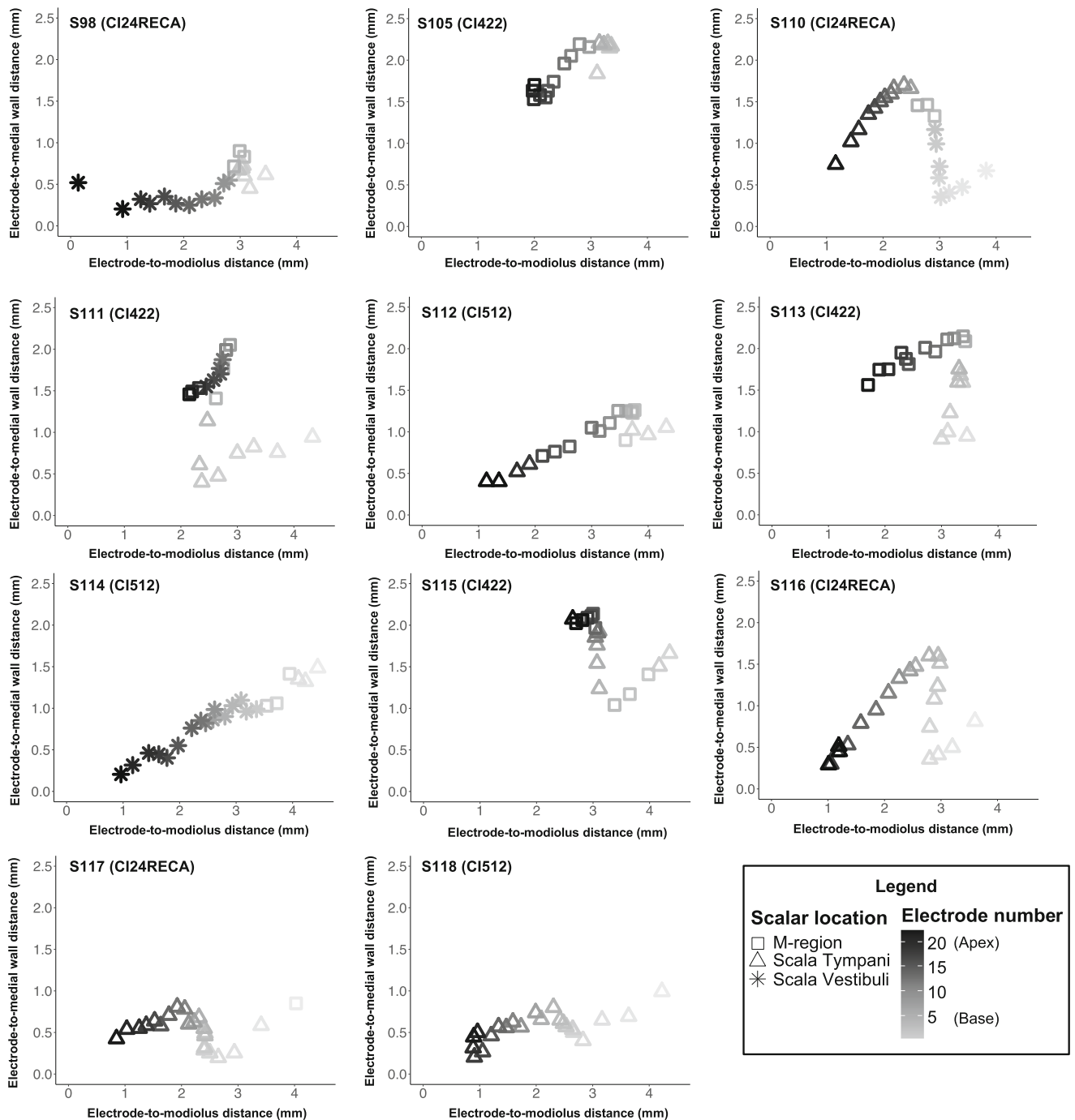


FIG. 2. For each subject, the electrode-to-mid modiolar (MMA) distance (mm) is plotted against the electrode-to-medial wall (MW) distance (mm). Scalar location is coded by symbol shape, and the gradient of black to gray coloring reflects basal-to-apical location (Electrode 1 = base; Electrode 22 = apex), respectively. The subject

identifier and electrode type are located within each figure. It should be noted that only those electrodes that were used for ECAP or psychophysical measurements are shown here. Those electrodes that were deactivated in the clinical maps are not shown

provided in Table 3. Note that in keeping with previous studies, we found that ECAP AGF slopes and thresholds for 7 and 30 μ s IPG are highly correlated with one another ($r=0.948$, $p<0.001$) and therefore in order to reduce multiple comparisons, only data for the 7 μ s IPG condition are formally assessed in the paper. Please refer to Table 4 for

correlation matrix showing interrelationships between dependent variables measured in the study. The summary findings of all linear mixed model analyses are provided in Table 5.

Overall, the results showed that both ECAP thresholds and AGF linear slopes were significantly related to MMA distance and that neither the IPG Effect for

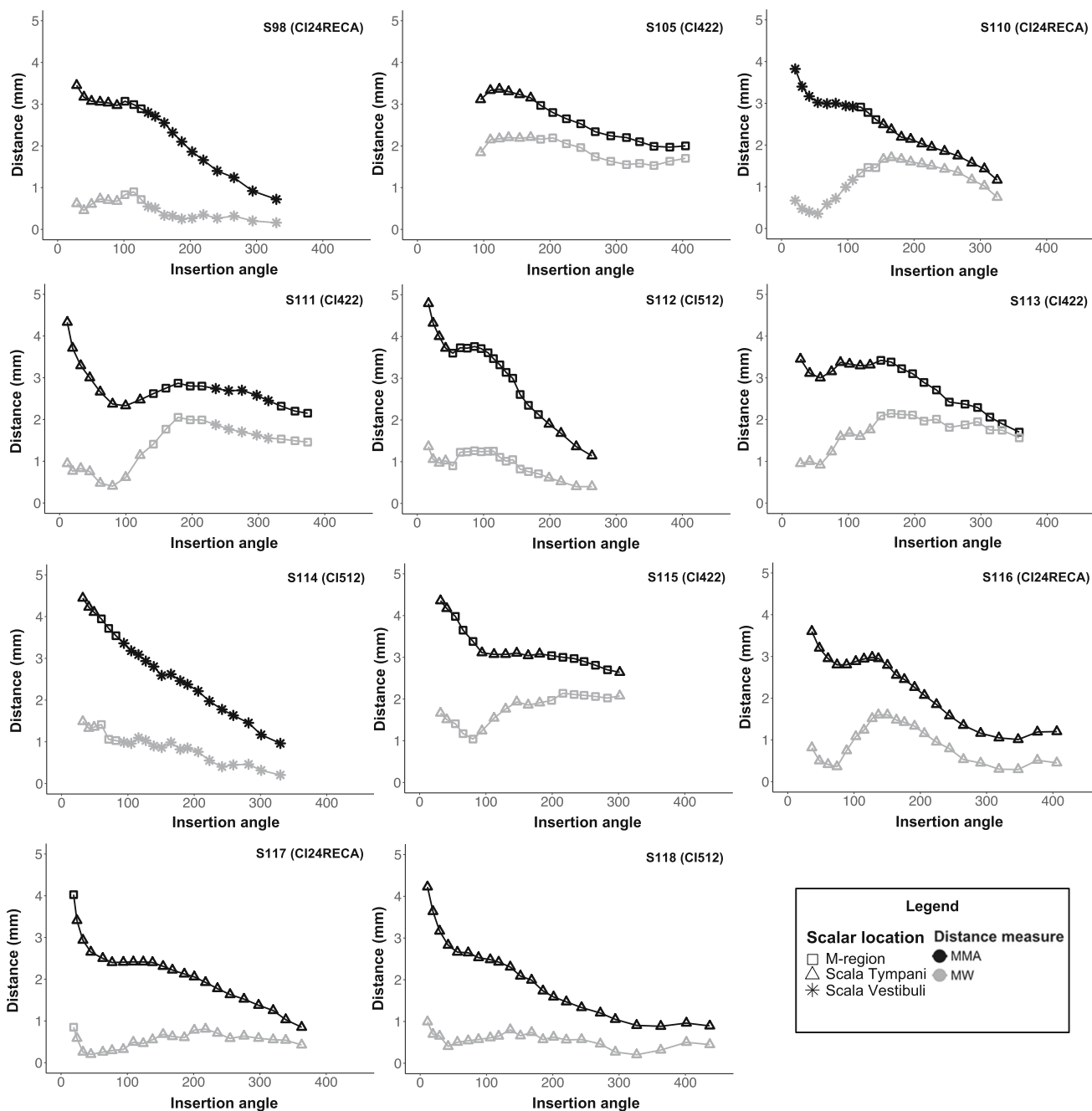


FIG. 3. For each subject, the electrode-to-mid modiolar (MMA) distance (black symbols) and electrode-to-medial wall (MW) distance (gray symbols) (mm) are plotted against insertion angle. All other details are similar to those described for Fig. 2

the ECAP AGF linear slope nor threshold was related to either distance measure. The relationship between ECAP thresholds for a 7 μ s IPG stimulus and MMA or MW distances are shown in Fig. 5 a and b, respectively. As noted in the figure legend, dashed and solid lines for Figs. 5 through 11 represent significance at the level of individual linear regressions within each subject. Specifically, we separately performed least-squares linear regression analysis between the independent and dependent variable in question for each

subject. Although the raw statistical data are not reported here, solid and dashed lines represent a significant ($p < 0.05$) and non-significant ($p \geq 0.05$) relationships. Such analyses were performed to better visually represent the data and to show within-subject relationships; however, the linear mixed model remains the focus of statistical interpretation.

Results of the linear mixed model analyses revealed that both models were significant (MMA: $t(8.84) = 3.318$, $p = 0.009$; MW: $t(11.35) = 3.337$, $p = 0.006$), sug-

TABLE 3

Descriptive statistics (average, standard deviation, minimum and maximum values) for the primary independent and dependent variables of interest in the study. The average and standard deviation values represent calculations across all subjects. The “min” and “max” values represent either the lowest or highest averaged response for one subject, when averaged across the electrodes in a single subject. Thus, the average across-values shown for the “min” and “max” rows represent a single subject with the lowest or highest values, when averaged across the array, for each measure

	<i>Psychophysical detection threshold- 80 pps (dB re:1 mA)</i>	<i>Multipulse Integration</i>	<i>ECAP AGF linear slope-7 μs IPG</i>	<i>ECAP AGF linear slope- IPG Effect</i>	<i>ECAP threshold-7 μs IPG</i>	<i>ECAP threshold-PG Effect</i>	<i>Medial-lateral distance (MW) in mm</i>	<i>Medial-lateral distance (MMA) in mm</i>
Average (All subjects)	-11.70	-1.15	0.62	0.12	-8.65	-1.23	1.10	2.57
Standard Deviation (All subjects)	0.62	0.37	0.18	0.09	1.64	0.61	0.33	0.66
Min across-site average (1 subject)	-7.34	-0.14	0.36	0.01	-5.82	-0.79	0.48	1.94
Max across-site average (1 subject)	-15.03	2.11	1.37	0.38	-12.48	-1.93	1.91	3.23

gesting that ECAP threshold values systematically increased with an increase in MMA or MW distance. The maximum likelihood revealed a significant difference between the two models ($\chi^2 = 76.55$, $p < 0.001$). Based on the AIC value, the MMA measure yields a better model and suggests that the ECAP threshold increased by 1.47 dB for every 1-mm increase in MMA distance. The relationship between the IPG Effect for ECAP thresholds and MMA or MW distances are shown in Fig. 6a and b, respectively.

Results of the linear mixed model analysis revealed that the model for both MMA ($t(9.00) = -0.279$, $p = 0.786$) and MW ($t(9.62) = -0.105$, $p = 0.918$) medial-lateral distance measures were non-significant.

The relationship between ECAP AGF linear slope for a 7 μ s IPG stimulus and MMA or MW distance are shown in Fig. 7a and b, respectively. Results of the linear mixed model analyses revealed that only one model was significant (MMA: $t(10.29) = -2.334$, $p = 0.04$), suggesting that ECAP AGF linear slope values

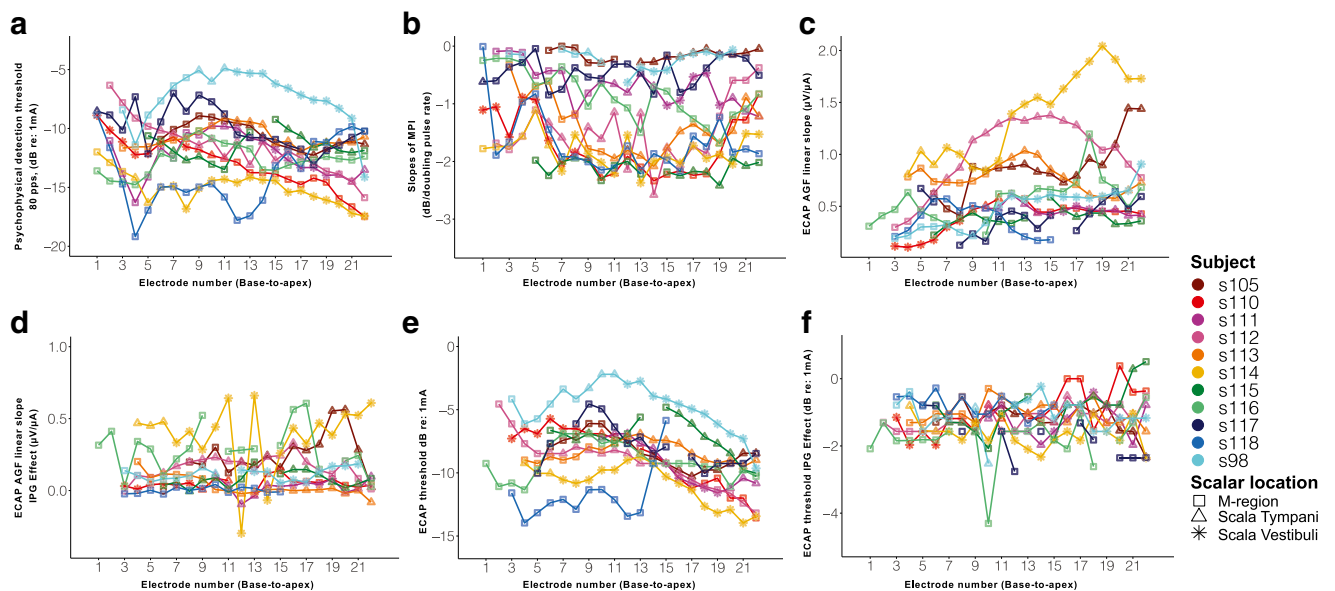


FIG. 4. Line graphs showing individual raw data for each subject, at each electrode site (1–22, base to apex) for each of the primarily dependent variables of interest examined in the current study: **a** Psychophysical detection thresholds at 80 pps; **b** MPI slopes; **c** ECAP

AGF linear slopes; **d** ECAP AGF linear slope IPG Effect; **e** ECAP thresholds; and **f** ECAP thresholds IPG Effect. Scalar location is coded by symbol shape and is consistent with symbols used in Fig. 2. Each subject is shown in a different color

TABLE 4

Correlational matrix (Pearson product-moment correlation analysis) for all dependent variables assessed in the study, even those not examined as primary outcome measures in the study (e.g., 640 pps psychophysical detection thresholds). Significant correlations are shown with an asterisk (* $p < 0.05$; ** $p < 0.01$; *** $p < 0.001$)

	Psychophysical detection threshold-80 pps (dB re:1 mA)	Psychophysical detection threshold-640 pps (dB re:1 mA)	Multipulse integration	ECAP AGF linear slope- 7 μ s IPG	ECAP AGF linear slope-30 μ s IPG	ECAP AGF linear slope- IPG Effect	ECAP threshold- 7 μ s IPG	ECAP threshold- 30 μ s IPG	ECAP threshold- IPG Effect
Psychophysical detection threshold- 80 pps (dB re:1 mA)	–	0.840***	0.356***	–0.259***	–0.249	–0.165	0.889***	0.819***	–0.034
Psychophysical detection threshold- 640 pps (dB re:1 mA)	0.840***	–	0.786***	–0.259***	–0.235***	–0.075	0.688***	0.642***	–0.113
Multipulse Integration	0.356***	0.786***	–	–0.166*	–0.136	0.061	0.227**	0.221**	–0.162*
ECAP AGF linear slope- 7 μ s IPG	–0.259***	–0.259***	–0.166*	–	0.948***	0.499***	–0.355***	–0.355***	–0.163*
ECAP AGF linear slope- 30 μ s IPG	–0.249***	–0.235***	–0.136	0.948***	–	0.695***	–0.329***	–0.392***	–0.163*
ECAP AGF linear slope- IPG Effect	–0.165	–0.075	0.061	0.499***	0.695***	–	–0.166*	–0.230**	–0.254**
ECAP threshold- 7 μ s IPG	0.889***	0.688***	0.227**	–0.355***	–0.329***	–0.166*	–	0.918***	–0.110
ECAP threshold- 30 μ s IPG	0.819***	0.642***	0.221**	–0.355***	–0.392***	–0.230**	0.918***	–	0.171*
ECAP threshold- IPG Effect	–0.034	–0.113	–0.162*	–0.163*	–0.163*	–0.254***	–0.110	0.171*	–

TABLE 5

Summary of results from linear mixed modeling examining relationship between each electrophysiological and psychophysical measure and medial-lateral electrode location. The specific measure is provided in the first column, the best model for predicting the relationship with each measure is in the second column, and the figure that shows the model is shown in the third column

Measure	Relationship to medial-lateral distance	Figure
ECAP threshold	Best model: MMA (1.47 dB per mm)	5
ECAP threshold IPG Effect	No significant model	6
ECAP AGF linear slope	Best model: MMA ($-0.12 \mu\text{V}/\mu\text{A}$ per mm)	7
ECAP AGF linear slope IPG Effect	No significant model	8
Psychophysical detection threshold	Best Model: MMA (0.96 dB per mm)	9
Psychophysical MPI slope	No significant model	10

systematically decreased with increasing MMA distance. Specifically, the fitted model suggests that ECAP AGF slope decreased by $0.12 \mu\text{V}/\mu\text{A}$ for every 1 mm increase in MMA distance.

Figure 8a and b show the relationship between ECAP AGF linear slope IPG Effect and MMA or MW distance measures, respectively. Linear mixed modeling analyses revealed that neither the MMA ($t(12.45) = -0.462$, $p = 0.64$) nor the MW distance measure models ($t(7.66) = -0.709$, $p = 0.49$) was significant. These results suggest that the ECAP AGF linear slope IPG Effect was relatively independent of distance between the electrode and presumed location of stimulated neural population.

Relation of Electrode Locations to Psychophysical Measures

In keeping with the ECAP data reported above, the across-site patterns for psychophysical measures of interest for each subject are shown in Fig. 4a and b, and the descriptive statistics are provided in Table 3. We found that psychophysical detection thresholds for 80 and 640 pps are highly correlated with one

another ($r = 0.840$, $p < 0.001$) and only data for the 80 pps condition are formally assessed in the paper (Table 4).

Results for all psychophysical measures revealed that psychophysical detection thresholds were related to medial-lateral electrode distance, but MPI slopes were not. Figure 9 and b show that both MMA and MW distance measures appear to be related to psychophysical thresholds for a low pulse rate (80 pps) stimulus. However, linear mixed modeling revealed that the MW distance was not related to detection thresholds ($t(9.35) = 1.897$, $p = 0.08$), but the MMA measure was significantly related to psychophysical detection thresholds across the electrode array ($t(11.42) = 3.044$, $p = 0.01$). This model suggests that psychophysical detection thresholds for the low-rate (80 pps) biphasic pulse train increased by 0.96 dB for every 1-mm increase in MMA distance.

Figure 10 demonstrates the relationship between electrode distance and the slope of the MPI function. Linear mixed modeling showed that neither the distance to the MMA ($t(11.11) = 0.878$, $p = 0.39$) nor the distance to the MW ($t(10.98) = -2.241$, $p = 0.08$) was significant predictor of MPI slopes across subjects

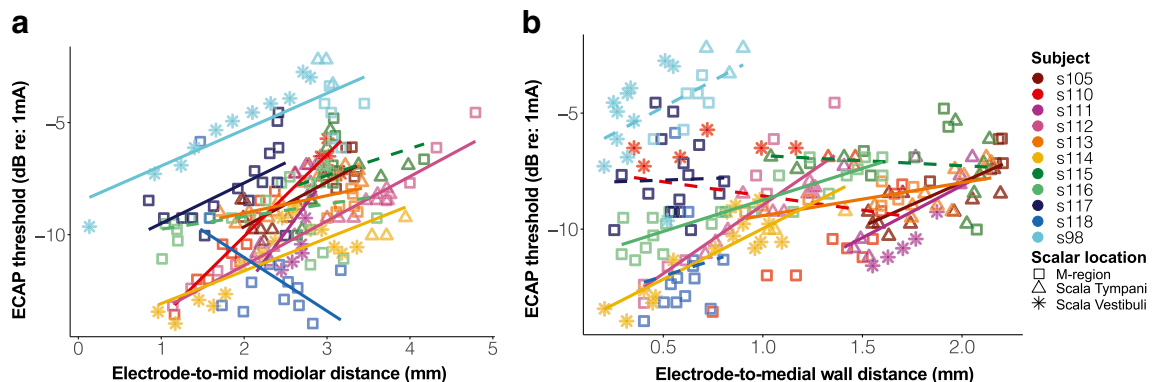


FIG. 5. Scatterplot showing the relationship, for each subject, between ECAP thresholds dB re: 1 mA (7 μs IPG condition) and medial-lateral electrode position. **a** The electrode-to-mid modiolar distance (MMA); **b** the electrode-to-medial wall distance (MW). Scalar location is coded by symbol shape and is consistent with symbols used in Fig. 2. Each subject is shown in a different color.

Although not used for statistical interpretation of the data, solid lines represent significant least-squares regression analysis ($p < 0.05$) between the two variables for each subject, while dashed lines represent non-significant regression analyses ($p > 0.05$). These are shown in order to visually represent the data

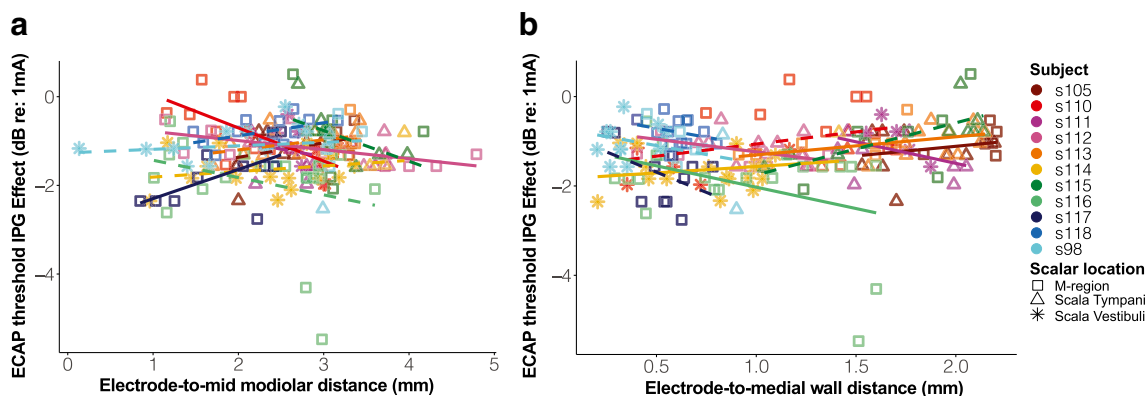


FIG. 6. Same as Fig. 5 but for the ECAP threshold (dB re: 1 mA) IPG Effect

(Fig. 10a and b). Similar to the ECAP AGF linear slope and threshold IPG Effect, these results suggest that MPI slopes for each electrode were independent of the distance between the electrode and stimulated neural fibers.

Comparison of MPI and ECAP IPG

Previous studies in animals have shown that both MPI and the ECAP AGF linear slope IPG Effect are (1) related to neural density in cochlear-implanted guinea pigs and (2) are related to speech recognition performance in bilaterally implanted human subjects (Pfungst et al., 2011; Zhou and Pfungst, 2014; Pfungst et al., 2017; Schwartz-Leyzac and Pfungst, 2018; Schwartz-Leyzac et al., 2019; Schwartz-Leyzac et al., Submitted). Hence it is logical that these two measures might be correlated with one another. A linear mixed model approach was used to assess this hypothesis; however, results (shown in Fig. 11) suggest no significant relationship between these two functional health measures ($t(5.02) = -1.242$, $p = 0.26$). These results suggest that, although both measures appear to somewhat reflect conditions of neural health, the specific underlying mechanism appears to be quite different. However, neither of these appear to be related to electrode location.

DISCUSSION

The present study examined how medial-lateral distance of the CI electrode array affects psychophysical and electrophysiological measures that have been shown previously to reflect neural conditions in cochlear implanted animals. Results from the present study revealed that ECAP thresholds and AGF linear slopes, when measured within each subject, were related to distances between the electrodes and the MMA (Figs. 5a and 7a and Table 5). Specifically, ECAP thresholds increased and AGF linear slopes decreased, with increasing distance between the electrode and the MMA based on analysis using a within-subject, mixed model approach. These results are somewhat consistent with previous literature. DeVries et al. (2016) reported no relationship between ECAP amplitude (measured with a moderately loud stimulus level) and distance between the electrode and medial wall (DeVries et al., 2016). Although in the present study we examined the ECAP AGF linear slope, and not amplitude, previous results in humans suggest that both of these suprathreshold measures are often related with one another (Schwartz-Leyzac and Pfungst, 2016) and reflect SGN density in animal models (Ramekers et al., 2014; Pfungst et al., 2017; Schwartz-Leyzac et al., Submitted).

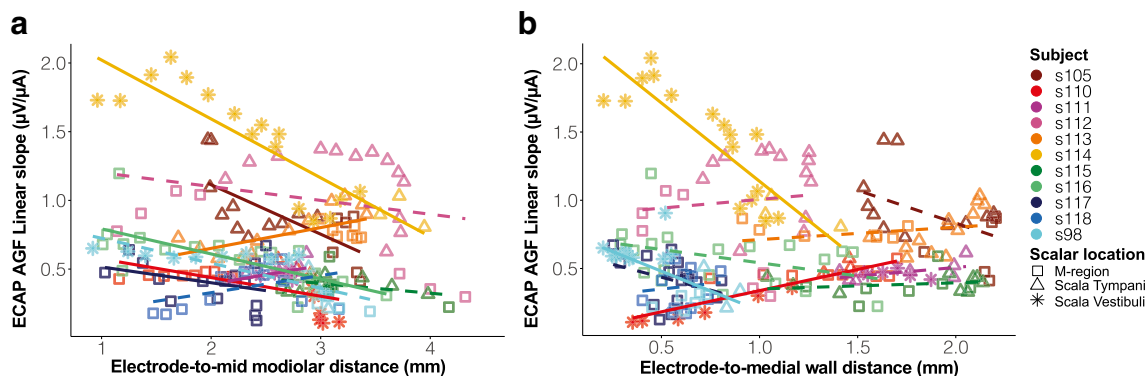


FIG. 7. Same as Fig. 5 but for the ECAP AGF linear slope ($\mu\text{V}/\mu\text{A}$), 7 μs IPG condition

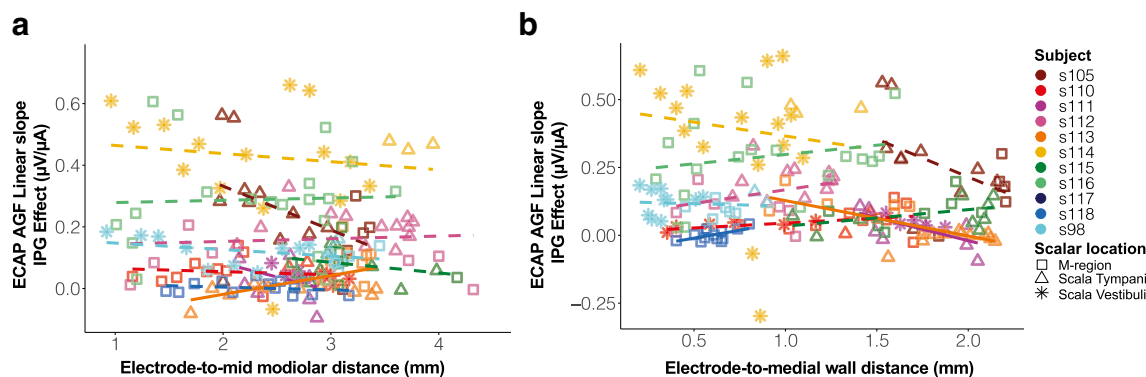


FIG. 8. Same as Fig. 5 but for the ECAP AGF linear slope IPG Effect

These results suggest that, at least when examining the relationship within each subject, both the ECAP threshold and AGF linear slope are related to the distance between the electrode and mid-modiolar axis but not necessarily the medial wall. Based on these results, one could infer that the site of excitation for residual SGNs occurs more central in the modiolus and is not restricted to the more peripheral portion of neurons (if present) adjacent to the medial wall of the cochlea.

The within-subject best model shown in the present study suggests that ECAP thresholds worsen with increasing MMA distance. Previous studies have shown poorer (higher) ECAP thresholds in the base compared with the apex (Nehme et al., 2014; Lathuilliere et al., 2017) and Shepherd et al. (1993) showed that ABR Wave IV thresholds decrease (improve) with decreased medial-lateral distance. Logically, base-to-apex variation in ECAP measures could be attributed to a gradient of neural degeneration, medial-lateral position of the electrodes from apex to base, or both of these factors (Hinojosa and Marion, 1983; Nadol, 1997). Therefore, it is possible that factors such as base-to-apex changes in anatomy and neural structure due to deafness could also be influencing the ECAP AGF linear slope and threshold measures (Hinojosa and Marion, 1983; Nadol, 1997). The results shown in the present study (e.g., ECAP

AGF linear slopes decrease with increasing MMA distance) contradict those previously observed by Shepherd and colleagues in the animal model (Shepherd et al., 1993) who reported that EABR Wave IV AGF linear slopes increase with increasing medial-lateral distance. While the reason for such a discrepancy is not clear, it is possible that covarying factors (e.g., base-to-apex neural health and medial-lateral electrode location) in human subjects obscure the relationship observed in a controlled animal model in which responses are located on a single electrode and/or location. Future studies should examine the relationship between medial-lateral distance and ECAP measures across subjects using a fixed electrode location or insertion angle to more accurately assess these questions.

Previous studies using focused stimulation by either phased-array stimulation (Long et al., 2014) or steered-quadrupolar configuration (DeVries et al., 2016) showed that psychophysical detection thresholds increased with increasing distance between the electrode and cochlear medial wall. In the present study, it was observed that psychophysical thresholds using a monopolar configuration were significantly and positively related to MMA distance, but not distance to the medial wall (MW distance). Although the current study did not examine a narrower electrode configuration for comparison, results reported by Long et al. (2014) also

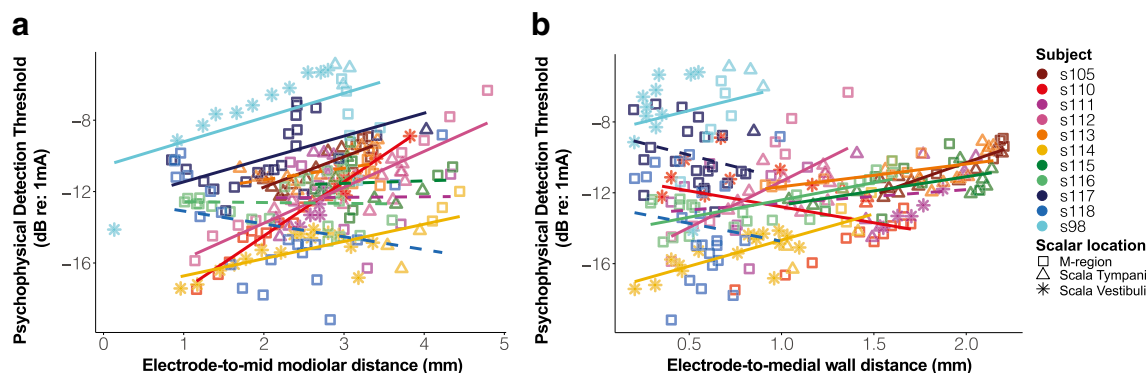


FIG. 9. Same as Fig. 5 but for psychophysical detection thresholds (dB re: 1 mA, 80 pps)

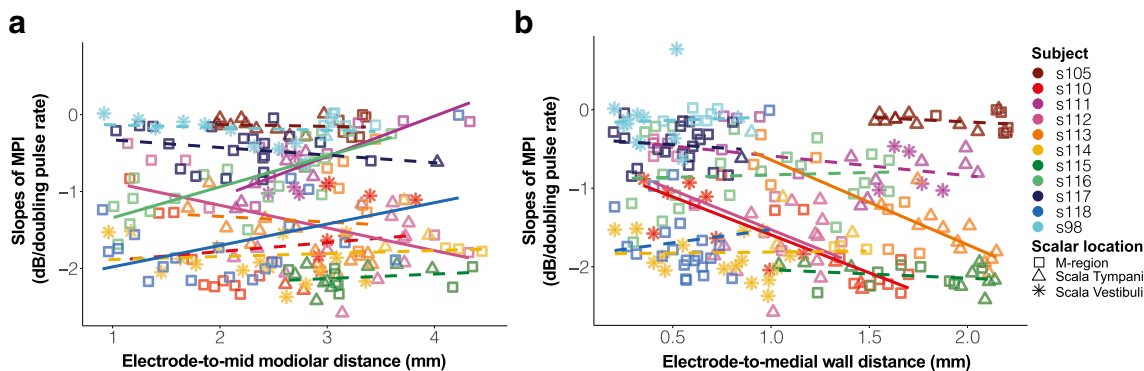


FIG. 10. Same as Fig. 5 but for the multipulse integration (MPI) slopes

performed comparative measures using a monopolar stimulation mode in some subjects, and results showed that the detection thresholds using a monopolar configuration did not often significantly reflect distance between the electrode and the medial wall. That particular study did not examine the MMA measure used here. The current path for a monopolar stimulation mode is not certain and likely varies for each CI recipient, but it likely creates a broader excitation pattern that extends to extra-cochlear structures and may affect intra-cochlear excitation patterns as well. The present findings for psychophysical detection thresholds suggest that, similar to results obtained using ECAP measures, the site of excitation is not necessarily adjacent to the medial wall but is located more central in the modiolar core. It is logical that for a more focused stimulation, the current is more localized and represents activation of local neural fibers. In fact, studies have shown greater variance in psychophysical detection thresholds across electrode sites in an array for more focused, rather than broad, electrode configurations (Pfungst et al., 2004; Bierer, 2007). Thus, these studies argued that narrow excitation patterns are observed for focused compared with broad electrode configurations.

Further studies are needed in a controlled animal model to better understand how electrode configuration interacts with neural conditions to determine neural activation and sensitivity. In theory, SGN

degeneration associated with significant hearing loss and the deafening process could result in a change of site of excitation. Specifically, there is some evidence at least in animals that the peripheral process of SGN fibers degenerate towards the cell body, however often at the same rate as degeneration of the cell body itself (Wise et al., 2017). Results in humans show that degeneration of the peripheral process can be independent of the associated cell body; however, this findings varies across ears, and the specific rate of degeneration for both the peripheral process and cell body is unknown but appears to be quite slow (Hinojosa and Marion, 1983; Felix et al., 2002).

In keeping with our hypothesis, results showed the ECAP IPG Effect for AGF linear slope and threshold and MPI slopes are independent of medial lateral distance using the MMA or MW measure. In animal models, the IPG Effect for linear slope and MPI slopes have been shown to strongly correlate with SGN density in cochlear implanted guinea pigs; the IPG Effect for ECAP thresholds is also weakly correlated (Pfungst et al., 2011; Ramekers et al., 2014; Pfungst et al., 2015b; Schwartz-Leyzac et al., Submitted), and it is logical that these measures would be relatively independent of electrode location. Two of these measures (IPG Effect for AGF slope and MPI slopes) have also been shown to relate to speech recognition abilities in cochlear implanted humans (Zhou and Pfungst, 2014; Schwartz-Leyzac and Pfungst, 2018).

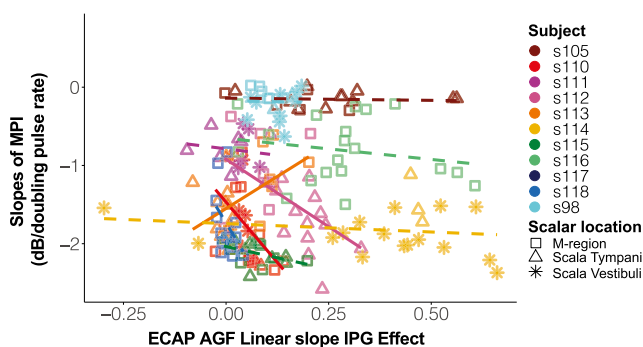


FIG. 11. Scatterplot showing the relationship, for each subject, between the ECAP AGF linear slope IPG Effect and MPI slopes. All other details are identical to those described for Fig. 5

Results from Schwartz-Leyzac and Pfingst (2018) demonstrated that the ECAP linear slope IPG Effect was a better predictor of speech recognition performance when compared with ECAP AGF linear slopes calculated using a constant IPG. It is possible that this finding was due, at least in part, to the fact that the latter measurement is affected by electrode position (see Fig. 7a) as well as neural conditions. Therefore, the IPG Effect could be a promising measure for clinical applications as it is independent of electrode position and reflects SGN health.

Although both the IPG Effect for ECAP AGF linear slope and MPI slopes have been shown to reflect neural health and relate to speech recognition abilities, results from the present study reveal that, within each subject, these measures are not related to one another (see Fig. 11). This finding suggests that, while both measures are correlated with SGN density in the cochlea, the underlying mechanisms may be different. It is hypothesized that MPI slopes represent temporal integration characteristics of SGNs, at least for pulse rates below 1000 pps, and MPI slopes also seem to depend on both SGN density and presence/absence of inner hair cells (Kang et al., 2010; Pfingst et al., 2011). The IPG sensitivity mechanism is complex and logically involves the ability of the neuron to recover from depolarization or hyperpolarization caused by the first phase of the biphasic pulse, before responding to the second phase in the opposite manner. It has been hypothesized that IPG sensitivity is also dependent on pulse shape, and neural health and anatomy might affect this if the population of neurons is primarily excited by the cathodic or anodic phase (Rattay, 1999; Rattay et al., 2001). In the current study, we used a cathodic-leading, biphasic pulse with a forward-masking artifact cancelation method to measure ECAP responses. Because most studies have shown that the anodic phase is the primary excitatory phase for most cochlear implanted adults (Undurraga et al., 2010; Schwartz-Leyzac and Pfingst, 2016; Hughes et al., 2017; Carlyon et al., 2018; Hughes et al., 2018; Jahn and Arenberg, 2019), we generally observe that ECAP AGF linear slopes increase with an increase in IPG duration (Schwartz-Leyzac and Pfingst, 2016, 2018). Taken together, it can be hypothesized that MPI slopes represent the ability of the auditory nerve to integrate multiple, biphasic pulses over a longer period of time (200–300 ms), while the IPG Effect represents the ability of the auditory nerve (or single neuron) to integrate, then recover from, an electrical current charge over one phase of a biphasic pulse. Given that each of these measures have been previously shown to independently correlate with speech recognition (Zhou and Pfingst, 2014; Schwartz-Leyzac and Pfingst, 2018) but seemingly represent distinct

attributes of neural health, future studies could examine how both factors help to explain variance in speech recognition abilities using a multiple regression approach.

Although the MMA and MW measures appear to be independent, it should be considered that they are related to some extent and that this relationship does vary based on the implant recipient's particular anatomy (as shown in Figs. 2 and 3). It should also be noted that the MMA measure does not completely represent the exact center of the modiolar core since the modiolar anatomy is not linear and completely symmetric from base to apex. However, the data shown in Fig. 3 for the MMA measure are fairly monotonic and do not appear to be biased, which might occur if the MMA was highly asymmetrical within the modiolus core. The results of the present study suggest that the MMA measure was more highly correlated with suprathreshold ECAP measures or psychophysical measures using monopolar stimulation, than the MW measure.

Overall, results from the present study suggest that multiple factors contribute to psychophysical detection thresholds and ECAP responses in cochlear implanted humans. The present study showed that, at least for monopolar stimulation, behavioral threshold detection and ECAP measures are at least somewhat dependent on medial-lateral electrode location. The MPI slopes and ECAP AGF linear slope IPG Effect were independent of electrode position. Scalar location was not specifically analyzed, but obvious patterns were not observed. Similarly, other studies have reported that scalar location does not seem to be strongly correlated with measures hypothesized to reflect SGN health (DeVries et al., 2016; Jahn and Arenberg, 2019). The results have important application for use in the clinical setting. Ideally, neural health measures that are relatively independent of electrode position (e.g., MPI slopes or ECAP IPG Effect) are ideally suited for use across a population of human subjects with varying electrode types and positions. However, a sufficient ECAP slope cannot always be calculated in human subjects (see Table 2), and therefore this particular ECAP measure might have a more limited clinical utility. Further studies are needed in order to better evaluate the potential application of both measures in the clinical setting to improve speech recognition outcomes.

ACKNOWLEDGMENTS

We would like to thank the subjects for their participation in the research, and we are grateful to the University of Michigan Cochlear Implant team for their support and assistance with subject recruitment.

Funding Information These studies were funded by NIH NIDCD R01DC015809 and a University of Michigan MCubed grant.

COMPLIANCE WITH ETHICAL STANDARDS

Conflict of Interest The authors declare that they have no conflict of interest.

Publisher's Note Springer Nature remains neutral with regard to jurisdictional claims in published maps and institutional affiliations.

REFERENCES

- ABBAS PJ, HUGHES ML, BROWN CJ, MILLER CA, SOUTH H (2004) Channel interaction in cochlear implant users evaluated using the electrically evoked compound action potential. *Audiol Neuro-otol* 9:203–213
- ABBAS PJ, BROWN CJ, SHALLOP JK, FIRSZT JB, HUGHES ML, HONG SH, STALLER SJ (1999) Summary of results using the nucleus CI24M implant to record the electrically evoked compound action potential. *Ear Hear.* 20:45–59
- BATES D, MAECHLER M, BOKER B, WALKER S (2015) Fitting linear mixed-effects models using lme4. *J. Stat. Softw.* 67:1–48
- BIERER JA (2007) Threshold and channel interaction in cochlear implant users: evaluation of the tripolar electrode configuration. *J Acoustic Soc Am* 121:1642–1653
- BIERER JA, FAULKNER KF (2010) Identifying cochlear implant channels with poor electrode-neuron interface: partial tripolar, single-channel thresholds and psychophysical tuning curves. *Ear Hear.* 31:247–258
- CARLYON RP, COSENTINO S, DEEKS JM, PARKINSON W, ARENBERG JA (2018) Effect of stimulus polarity on detection thresholds in cochlear implant users: relationships with average threshold, gap detection, and rate discrimination. *J Assoc Res Otolaryngol*
- DEVRIES L, SCHEPERLE R, BIERER JA (2016) Assessing the electrode-neuron interface with the electrically evoked compound action potential, electrode position, and behavioral thresholds. *J. Assoc. Res. Otolaryngol.* 17:237–252
- EARL BR, CHERTOFF ME (2010) Predicting auditory nerve survival using the compound action potential. *Ear Hear.* 31:7–21
- FELIX H, POLLAK A, GLEESON M, JOHNSON LG (2002) Degeneration pattern of human first-order cochlear neurons. *Adv. Otorhinolaryngol.* 59:116–123
- FINLEY CC, HOLDEN TA, HOLDEN LK, WHITING BR, CHOLE RA, NEELY GJ, HULLAR TE, SKINNER MW (2008) Role of electrode placement as a contributor to variability in cochlear implant outcomes. *Otology & neurotology* : official publication of the American Otological Society, American Neurotology Society [and] European Academy of Otology and Neurotology 29:920–928
- GOLDWYN JH, BIERER SM, BIERER JA (2010) Modeling the electrode-neuron interface of cochlear implants: effects of neural survival, electrode placement, and the partial tripolar configuration. *Hear. Res.* 268:93–104
- HALL RD (1990) Estimation of surviving spiral ganglion cells in the deaf rat using the electrically evoked auditory brainstem response. *Hear. Res.* 49:155–168
- HE S, TEAGLE HFB, BUCHMAN CA (2017) The electrically evoked compound action potential: from laboratory to clinic. *Front. Neurosci.* 11:339
- HINOJOSA R, MARION M (1983) Histopathology of profound sensorineural deafness. *Ann. N. Y. Acad. Sci.* 405:459–484
- HUGHES ML, GOEHRING JL, BAUDHUIN JL (2017) Effects of stimulus polarity and artifact reduction method on the electrically evoked compound action potential. *Ear Hear.* 38:332–343
- HUGHES ML, CHOI S, GLICKMAN E (2018) What can stimulus polarity and interphase gap tell us about auditory nerve function in cochlear-implant recipients? *Hear. Res.* 359:50–63
- JAHN KN, ARENBERG JG (2019) Evaluating psychophysical polarity sensitivity as an indirect estimate of neural status in cochlear implant listeners. *J Assoc Res Otolaryngol* 20:415–430
- KANG SY, COLESA DJ, SWIDERSKI DL, SU GL, RAPHAEL Y, PFINGST BE (2010) Effects of hearing preservation on psychophysical responses to cochlear implant stimulation. *J Assoc Res Otolaryngol* 11:245–265
- KUZNETSOVA A, BROCKHOFF PB, CHRISTENSEN RHB (2017) lmerTest package: tests in linear mixed effects models. *J. Stat. Softw.* 82:1–26
- LATHUILLIERE M, MERKLEN F, PIRON JP, SICARD M, VILLEMUS F, MENJOT DE CHAMPFLEUR N, VENAIL F, UZIEL A, MONDAIN M (2017) Cone-beam computed tomography in children with cochlear implants: the effect of electrode array position on ECAP. *Int. J. Pediatr. Otorhinolaryngol.* 92:27–31
- LONG CJ, HOLDEN TA, MCCLELLAND GH, PARKINSON WS, SHELTON C, KELSALL DC, SMITH ZM (2014) Examining the electro-neural interface of cochlear implant users using psychophysics, CT scans, and speech understanding. *J Assoc Res Otolaryngol* 15:293–304
- NADOL JB JR (1997) Patterns of neural degeneration in the human cochlea and auditory nerve: implications for cochlear implantation. *Otolaryngol–Head Neck Surg* 117:220–228
- NEHME A, EL ZIR E, MOUKARZEL N, HAIDAR H, VANPOUCKE F, ARNOLD L (2014) Measures of the electrically evoked compound action potential threshold and slope in HiRes 90K(TM) users. *Cochlear implants international* 15:53–60
- PFINGST BE, XU L, THOMPSON CS (2004) Across-site threshold variation in cochlear implants: relation to speech recognition. *Audiol Neuro-otol* 9:341–352
- PFINGST BE, COLESA DJ, SWIDERSKI DL, RAPHAEL Y, SCHVARTZ-LEYZAC KC (2019) Using detection thresholds to estimate cochlear health: single pulse vs. multipulse stimuli. In: conference on implantable auditory prostheses. Lake Tahoe, CA
- PFINGST BE, HUGHES AP, COLESA DJ, WATTS MM, STRAHL SB, RAPHAEL Y (2015A) Insertion trauma and recovery of function after cochlear implantation: evidence from objective functional measures. *Hear. Res.* 330:98–105
- PFINGST BE, COLESA DJ, HEMBRADOR S, KANG SY, MIDDLEBROOKS JC, RAPHAEL Y, SU GL (2011) Detection of pulse trains in the electrically stimulated cochlea: effects of cochlear health. *J Acoustic Soc Am* 130:3954–3968
- PFINGST BE, COLESA DJ, SWIDERSKI DL, HUGHES AP, STRAHL SB, SINAN M, RAPHAEL Y (2017) Neurotrophin gene therapy in deafened ears with cochlear implants: long-term effects on nerve survival and functional measures. *J. Assoc. Res. Otolaryngol.* 18:731–750
- PFINGST BE, ZHOU N, COLESA DJ, WATTS MM, STRAHL SB, GARADAT SN, SCHVARTZ-LEYZAC KC, BUDENZ CL, RAPHAEL Y, ZWOLAN TA (2015B) Importance of cochlear health for implant function. *Hear. Res.* 322:77–88
- PRADO-GUITIERREZ P, FEWSTER LM, HEASMAN JM, MCKAY CM, SHEPHERD RK (2006) Effect of interphase gap and pulse duration on electrically evoked potentials is correlated with auditory nerve survival. *Hear. Res.* 215:47–55
- RAMEKERS D, VERSNEL H, STRAHL SB, KLIS SF, GROLMAN W (2015) Temporary neurotrophin treatment prevents deafness-induced auditory nerve degeneration and preserves function. *J. Neurosci.* 35:12331–12345
- RAMEKERS D, VERSNEL H, STRAHL SB, SMEETS EM, KLIS SF, GROLMAN W (2014) Auditory-nerve responses to varied inter-phase gap and

- phase duration of the electric pulse stimulus as predictors for neuronal degeneration. *J Assoc Res Otolaryngol* 15:187–202
- RATTAY F (1999) The basic mechanism for the electrical stimulation of the nervous system. *Neuroscience* 89:335–346
- RATTAY F, LUTTER P, FELIX H (2001) A model of the electrically excited human cochlear neuron: I. Contribution of neural substructures to the generation and propagation of spikes. *Hear. Res.* 153:43–63
- RCORETEAM (2018) R: a language and environment for statistical computing. Austria R Foundation for Statistical Computing, Vienna
- SCHVARTZ-LEYZAC KC, PFINGST BE (2016) Across-site patterns of electrically evoked compound action potential amplitude-growth functions in multichannel cochlear implant recipients and the effects of the interphase gap. *Hear. Res.* 341:50–65
- SCHVARTZ-LEYZAC KC, PFINGST BE (2018) Assessing the relationship between the electrically evoked compound action potential and speech recognition abilities in bilateral cochlear implant recipients. *Ear Hear.* 39:344–358
- SCHVARTZ-LEYZAC KC, COLESA DJ, BUSWINKA CJ, SWIDERSKI DL, RAPHAEL Y, PFINGST BE (2019) Changes over time in the electrically evoked compound action potential (ECAP) interphase gap (IPG) effect following cochlear implantation in guinea pigs. *Hear. Res.* 383:e1–e15
- SCHVARTZ-LEYZAC KC, COLESA DJ, BUSWINKA CJ, HUGHES AP, RAPHAEL Y, PFINGST BE (SUBMITTED) Estimating neural health using the electrically evoked compound action potential (ECAP) in chronically-implanted guinea pigs *The Journal of the Acoustical Society of America*
- SHEPHERD RK, JAVEL E (1997) Electrical stimulation of the auditory nerve. I. Correlation of physiological responses with cochlear status. *Hear. Res.* 108:112–144
- SHEPHERD RK, HATSUSHIKA S, CLARK GM (1993) Electrical stimulation of the auditory nerve: the effect of electrode position on neural excitation. *Hear. Res.* 66:108–120
- SKINNER MW, HOLDEN TA, WHITING BR, VOIE AH, BRUNSDEN B, NEELY JG, SAXON EA, HULLAR TE, FINLEY CC (2007) In vivo estimates of the position of advanced bionics electrode arrays in the human cochlea. *The Annals of otology, rhinology & laryngology Supplement* 197:2–24
- SMITH L, SIMMONS FB (1983) Estimating eighth nerve survival by electrical stimulation. *The Annals of otology, rhinology, and laryngology* 92:19–23
- TEYMOURI J, HULLAR TE, HOLDEN TA, CHOLE RA (2011) Verification of computed tomographic estimates of cochlear implant array position: a micro-CT and histologic analysis. *Otology & neurotology* : official publication of the American Otological Society, American Neurotology Society [and] European Academy of Otolology and Neurotology 32:980–986
- THE MATHWORKS I (2010) MATLAB. The MathWorks, Inc., Natick
- THE MATHWORKS I (2017) MATLAB. The MathWorks, Inc, Natick, Massachusetts, United States
- UNDURRAGA JA, VAN WIERINGEN A, CARLYON RP, MACHEREY O, WOUTERS J (2010) Polarity effects on neural responses of the electrically stimulated auditory nerve at different cochlear sites. *Hear. Res.* 269:146–161
- VAN DE HEYNING P, ARAUZ SL, ATLAS M, BAUMGARTNER WD, CAVERSACCIO M, CHESTER-BROWNE R, ESTIENNE P, GAVILAN J, GODEY B, GSTÖTTNER W, HAN D, HAGEN R, KOMPIS M, KUZOVKOV V, LASSALETTA L, LEFFEVRE F, LI Y, MÜLLER J, PARNES L, KLEINE PUNTE A, RAINE C, RAJAN G, RIVAS A, RIVAS JA, ROYLE N, SPRINZL G, STEPHAN K, WALKOWIAK A, YANOV Y, ZIMMERMANN K, ZOROWKA P, SKARZYNSKI H (2016) Electrically evoked compound action potentials are different depending on the site of cochlear stimulation. *Cochlear implants international* 17:251–262
- VAN EIJL RH, BUTTENHUIS PJ, STEGEMAN I, KLIS SF, GROLMAN W (2017) Systematic review of compound action potentials as predictors for cochlear implant performance. *Laryngoscope* 127:476–487
- VOIE AH (2002) Imaging the intact guinea pig tympanic bulla by orthogonal-plane fluorescence optical sectioning microscopy. *Hear. Res.* 171:119–128
- WISE AK, PUJOL R, LANDRY TG, FALLON JB, SHEPHERD RK (2017) Structural and ultrastructural changes to type I spiral ganglion neurons and Schwann cells in the deafened guinea pig cochlea. *J Assoc Res Otolaryngol* 18:751–769
- ZHOU N, PFINGST BE (2014) Relationship between multipulse integration and speech recognition with cochlear implants. *J Acoustic Soc Am* 136:1257
- ZHOU N, PFINGST BE (2016) Evaluating multipulse integration as a neural-health correlate in human cochlear-implant users: relationship to spatial selectivity. *J Acoustic Soc Am* 140:1537
- ZHOU N, XU L, PFINGST BE (2012) Characteristics of detection thresholds and maximum comfortable loudness levels as a function of pulse rate in human cochlear implant users. *Hear. Res.* 284:25–32
- ZHOU N, KRAFT CT, COLESA DJ, PFINGST BE (2015) Integration of pulse trains in humans and guinea pigs with cochlear implants. *J Assoc Res Otolaryngol* 16:523–534